Transmitting stepwise rotation between three molecule-gears on the Au(111) surface by STM

Kwan Ho Au Yeung, Tim Kühne, Frank Eisenhut, Michael Kleinwächter, Yohan Gisbert, Roberto Robles, Nicolas Lorente, Gianaurelio Cuniberti, Christian Joachim, Gwénaël Rapenne, et al.

Transmitting stepwise rotation between three molecule-gears on the Au(111) surface

Kwan Ho Au Yeung[1,2], Tim Kühne[1,2], Frank Eisenhut[1,2], Michael Kleinwächter[3], Yohan Gisbert[3], Roberto Robles[4], Nicolas Lorente[4,5], Gianaurelio Cuniberti[2], Christian Joachim[3], Gwénaël Rapenne[3,6], Claire Kammerer[3] and Francesca Moresco[1]*

[1]Center for Advancing Electronics Dresden, TU Dresden, 01062 Dresden, Germany

[2]Institute for Materials Science, TU Dresden, 01062 Dresden, Germany

[3]CEMES, Université de Toulouse, CNRS, 31055 Toulouse, France

[4]Centro de Física de Materiales CFM/MPC (CSIC-UPV/EHU), 20018 Donostia-San Sebastián, Spain

[5]Donostia international physics center, 20018 Donostia-San Sebastian, Spain

[6]Division of Materials Science, Nara Institute of Science and Technology, 8916-5 Takayama, Ikoma, Nara 630-0192, Japan

Corresponding Author

*Correspondence should be addressed to francesca.moresco@tu-dresden.de.

ABSTRACT

The realization of a train of molecule-gears working under the tip of a scanning tunneling microscope (STM) requires a stable anchor of each molecule to the metal surface. Such anchor can be promoted by a radical state of the molecule induced by a dissociation reaction. Our results, rationalized by density functional theory calculations, reveal that such open radical state at the cyclopentadiene core of star-shaped pentaphenylcyclopentadiene (PPCP) favors the anchoring. Furthermore, to allow the transmission of motion by STM manipulation, the molecule-gear should be equipped with specific groups facilitating the tip-molecule interactions. In our case, a *tert*-butyl group positioned at one tooth end of the gear benefits both the tip-induced manipulation and the monitoring of rotation. With this optimized molecular system we achieve reproducible and stepwise rotations of the single gears and transmit rotations up to three interlocked units.

KEYWORDS: molecular machine, gear, STM manipulation, on-surface synthesis, density functional theory

A molecular mechanical machine requires transmission of motions between active components (motors) and passive molecular structures (gears, pull-tabs) to become functional. These devices convert external excitations into rotation, where they can be triggered by light [1, 2,] chemical reactions [3], scanning tunneling microscope (STM) tips [4, 5, 6], or electric field [7]. While the advances in synthetic chemistry and on-surface chemistry allow the rational design of molecule-gears, the rotational mechanics and the corresponding transmission of motion remain a big challenge.

STM offers not only the real-space visualization of single molecules on surfaces, but also local manipulation as an external source of power, for examples, manipulating single molecules with the STM tip [8], driving nanocars by tunneling current and/or electric field [9, 10], turning on/off molecular switches [11, 12], and inducing chemical reactions [13, 14]. On this account, low-temperature STM in ultra-high vacuum (UHV) is an excellent tool for locally providing external input and monitoring the rotations of the molecule-gears under high-stability and clean-imaging conditions.

The first STM experimental study of a single molecule-rotor on a metal surface was performed in 1998 [15], showing lateral translations and continuous rotations of a single hexa-*tert*-butyl decacyclene (HB-DC) molecule on the Cu(100) surface at room temperature. Another breakthrough came several years later, in 2007, when a molecular rack-and-pinion device was demonstrated by using a low-temperature STM, known as the first interlocked molecular gear device [16], while the first complete rotation of a molecule-gear induced by STM manipulation was demonstrated in 2009 [5]. Recently, on a Pb(111) surface, the transmission of motion between two hexa-*tert*-butyl-pyrimidopentaphenylbenzene (HB-NBP) molecules mounted each on a single Cu adatom was demonstrated, using a third HB-NBP molecule as a "molecular handle" [17].

Furthermore, as an alternative strategy, promising results were presented with an individual molecule rotating via dipole-dipole interactions [18], or by surface-state mediated interaction [19, 20]. More examples on the rotation of molecule-gears with several strategies were single-molecule rotations on atomic axes [5, 21] and rotations of a gearing unit on top of molecular metallo-organic fragments (*i.e.* deckers or tripods) [22, 23]. Nonetheless, most of these cases are characterized by random (50% clockwise and 50% anticlockwise) directions of rotation, temperature-induced continuous rotation, or by the rotation of only one molecule. The challenges of a highly controlled transmission of rotation within a long train of molecule-gears are not yet resolved.

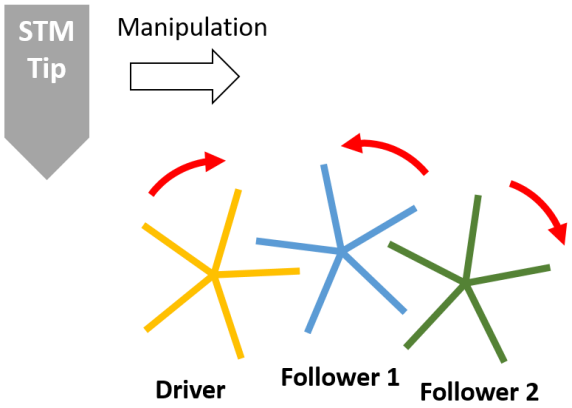

Figure 1. Illustration of a transmission of rotations between three star-shaped molecule-gears aligned on a metal surface. The interaction with the STM tip provides the mechanical energy to drive the first gear, namely the Driver gearing unit, so that this unit transmits the rotation to Follower 1 and 2.

Progressing toward a multi-gear assembly and the corresponding transmission of rotation, there are several key factors to be tackled: first, a strong anchoring is necessary for pinning individual molecule-gears at precise interlocking distances and rotating without any lateral displacements. Second, the tip-induced manipulation and the tip-molecule interaction have to be

optimized by choosing the appropriate parameters of tip-molecule distance and tunneling current and voltage [8]. Furthermore, a chemical or steric tag is beneficial for detecting the rotation by STM imaging. It is also crucial to consider the optimization for transmitting motion, like the length of the teeth or distance between the molecules. Figure 1 schematically illustrates the outline of the proposed system.

In this paper, we present two chemical modifications within the framework of a star-shaped pentaphenylcyclopentadiene (PPCP) molecule that takes a macroscopic gear as an analogy. As a proof-of-concept, STM lateral manipulation [24] was applied for investigating the stepwise rotations and the corresponding quality of anchors. As an example of a functional multi-gear system, we report on the stable transmission of motion along a train of three molecule-gears.

PPCP molecular fragments used in this study incorporate a central planar five-membered ring surrounded by five aromatic groups, thus exhibiting a star-shaped geometry. Anionic PPCP fragments have been intensely used as bulky ligands in organometallic chemistry, and coordination to the metal center can then occur from one, two, three or five carbon atoms located in the ring [25]. In the latter case, the flat and star-shaped PPCP ligand is symmetrically bonded to the metal center, while keeping a privileged rotational degree of freedom around the metal-cyclopentadiene axis. This arrangement has been previously exploited for ruthenium-based rotary molecule-machines, incorporating an additional tripodal scorpionate ligand as anchoring subunit in view of on-surface studies [22, 26].

In the present work, it was envisioned to anchor such star-shaped PPCP fragments directly on the Au(111) surface to construct a molecule-gear, after an homolytic cleavage of the C-Br bond present in the precursor. Interaction of the resulting radical state with the substrate would thus provide an anchoring point, ideally favoring rotary motions over translations. In order to monitor

the stepwise rotation of PPCP molecule-gears by STM, it appeared important to break the five-fold symmetry of the framework and incorporate a marker on one of the teeth. Two strategies have been devised: (1) substitution of a phenyl tooth by a pyrimidine group acting as a chemical tag (gear **1**), and (2) extension of one phenyl tooth with a *tert*-butyl group in *para* position, acting as a steric tag (gear **2**). The synthesis details are reported in the Methods section.

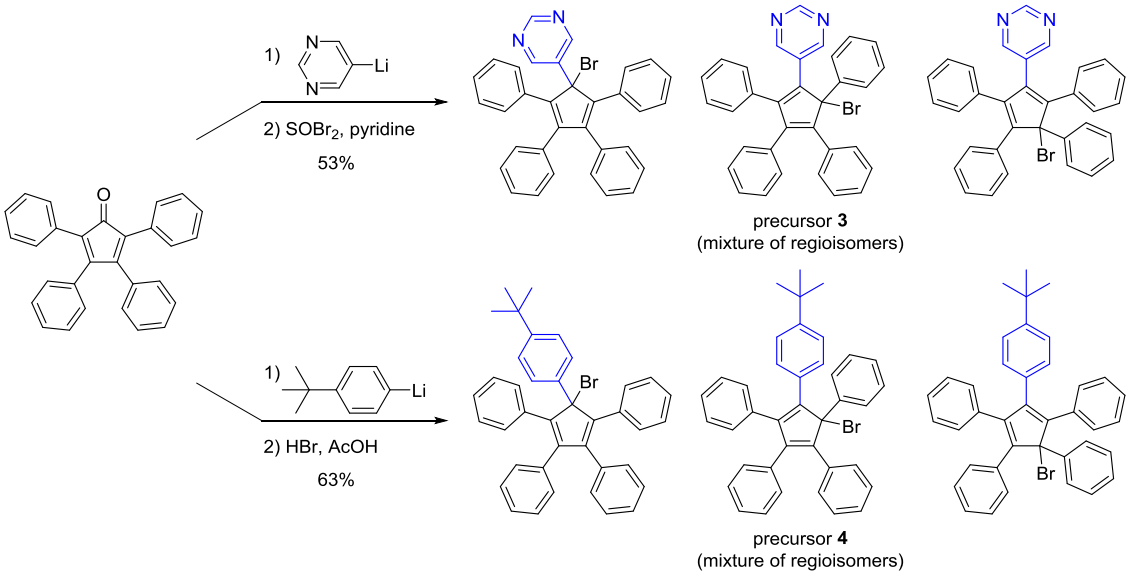

Scheme 1. Structure and synthesis of brominated precursors **3** and **4**, incorporating a pyrimidinyl chemical marker and a 4-*tert*-butylphenyl steric marker, respectively. Precursors **3** and **4** are obtained in two steps from 2,3,4,5-tetraphenylcyclopentadienone as a mixture of three regioisomers.

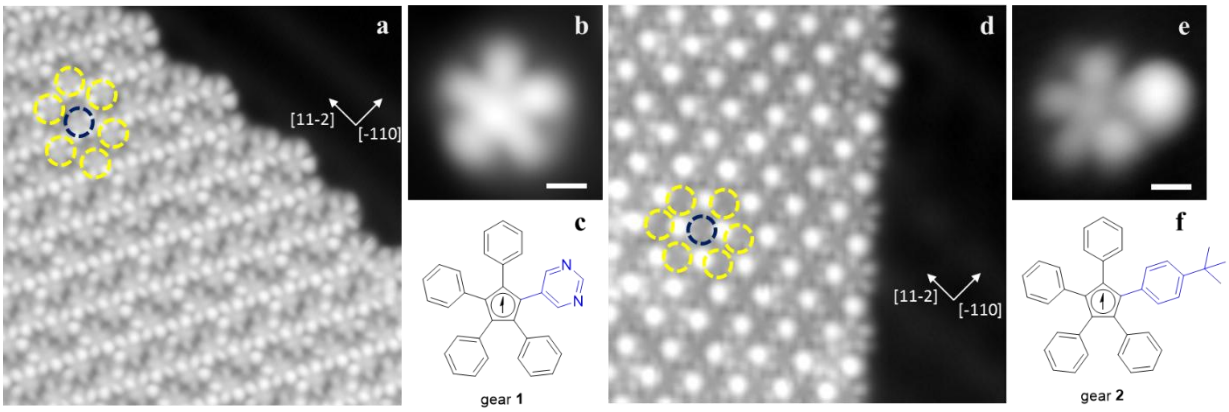

Figure 2. Overviews and the structure of molecule-gears on Au(111). (a – c) The structure of the PPCP-based gear **1** molecule, the black arrows represent the radical character of the molecule. the orientations of molecules. (a) Overview STM image (15 nm x 15 nm) taken at V = 500 mV and I = 7.2 pA. (b) STM image of a single gear **1** molecule. Scale bar = 0.5 nm. (c) Chemical structure of a gear **1** molecule. (d - f) The structure of the PPCP-based gear **2** molecule. (d) Overview STM image (15 nm x 15 nm) taken at V = 500 mV and I = 7.2 pA. (e) STM image of a single gear **2** molecule. Scale bar = 0.5 nm. (f) Chemical structure of a gear **2** molecule.

The deposition of the molecular precursors **3** and **4** (Scheme 1; as mixtures of regioisomers) on the Au(111) surface at sub-monolayer coverage was achieved by sublimation (see Methods section for details). As shown in the STM images of Figure 2a and d, we obtained close-packed molecular islands. Smaller islands or groups of a few molecules were also found at the elbows of the herringbone reconstruction of Au(111). Despite the use of precursor samples containing three regioisomers, the pattern of both monolayers appears homogeneous, which can be ascribed to the efficient thermal induced debromination upon sublimation of the three isomers leading to one single radical species on surface. For both designs, the gears form a lattice with six neighbors , as depicted with the dotted circles on Figures 2a and 2d. We assume that the interaction to the underlying substrate dominates the island formation, forcing the molecules to form a lattice with

six neighbors. This result in zigzag lines of interlocked molecules spaced too far to interlock between each other. The lattice is therefore C2 symmetry where two molecules occupy a unit cell. The nearest-neighbor distance of gear **1** is (1.21 ± 0.01) nm and of gear **2** is (1.36 ±0.02) nm. For comparison, from DFT relaxation we obtained a radius of the molecule around 0.78 nm including the tert-butyl group, or 0.65 nm without including it.

The brighter lobes in Figure 2d can be easily associated to the *tert*-butyl groups present in gear **2**, while the pyrimidine groups are not visible in the STM images of gear **1**.

The extraction of single molecules from an island to a clean Au(111) terrace was performed by a gentle STM tip crashing, but was not possible by STM lateral manipulation. On Figure 2e, STM images of single molecules reveal the expected chemical structure of gear **2** depicted on Figure 2f. This confirms that the *tert*-butyl group can act as a steric marker due to its distinguishable apparent height at about 0.22 nm, relatively higher than the planar phenyl ring at about 0.17 nm on the Au(111) surface. Importantly, such *tert*-butyl group can also be visualized under routine STM imaging condition (V = 500 mV and I = 10 pA), which is a key asset to track stepwise motions.

In the case of gear **1**, the single molecule image (Figure 2b) corresponds to the expected chemical star-shaped structure depicted on Figure 2c, with the five aryl teeth surrounding the central cyclopentadiene core. Even if pyrimidine moieties have already been successfully used as chemical markers in previous studies involving HB-NBP molecules, inducing contrast at bias voltage above 2.2 V on a Cu(111) surface [16], in our case on Au(111) we observed none of the mentioned features even by varying the bias voltage. The same absence of electronic tag effect was observed for the HB-NBP molecule on Pb(111) [17] suggesting that on Au(111) and Pb(111),

the pyrimidine moiety adopts a surface conformation that reduces its electronic interactions with the surface. This indicates that under such conditions we cannot exploit the pyrimidine group as a chemical tag.

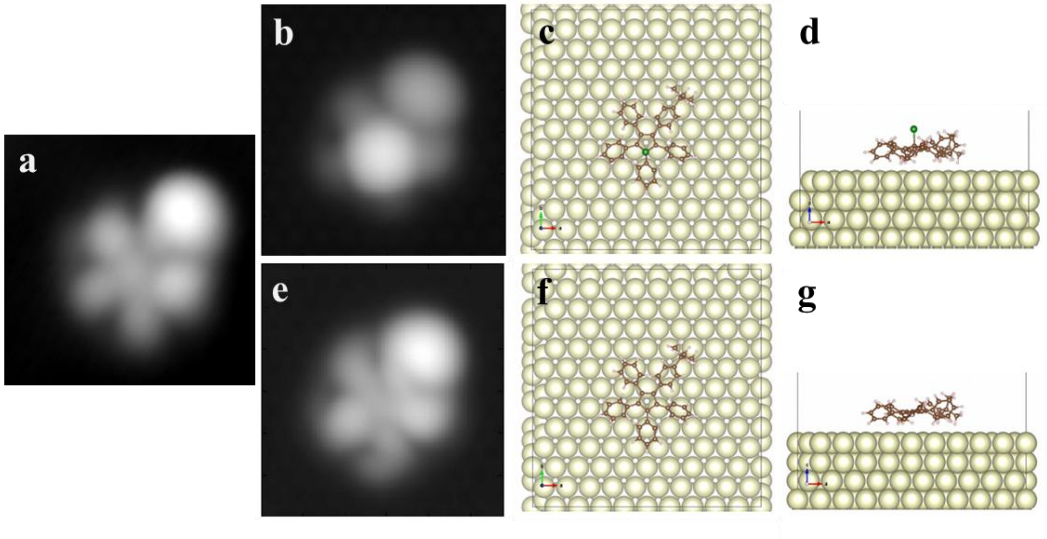

Figure 3. DFT simulations of brominated precursor **4** and radical state of molecule-gear **2** on Au(111). (a, b, e) Comparison of the experimental and simulated STM images. (a) Experimental image of a gear **2** molecule. The image (2.75 nm x 2.75 nm) was taken under V = 500 mV and I = 7.2 pA. (b) A simulated constant-current image of precursor **4** (one regioisomer) displaying a C-Br bond at the cyclopentadiene core. (e) A simulated image of gear **2** molecule after cleaving the C-Br bond at the core. The voltage bias of the simulations was V = 1.0 V. (c – d, f – g) Top and side views of the simulated adsorption geometries from (b) a precursor **4** and (e) gear **2** molecule.

Beside the presence of a tag to monitor a motion, another decisive property is to anchor individual molecule-gears on the surface so that their teeth can engage at a particular distance and the degrees of freedom along the gear train can be limited. A robust anchoring allows a stable rotational motion and limits the lateral displacement during manipulation. By analogy with

the coordination of PPCP rotary platforms to ruthenium centers in organometallic molecular machines [22, 27], we envisioned to anchor the PPCP gears on the Au(111) substrate via carbon-metal bonds. To this aim, the precursors molecules (see SI for details) incorporate a bromine atom on the central ring, since this halogen affords a good balance between precursors stability and ease of homolytic carbon-halogen bond cleavage. As known from previous literature [28], during sublimation of the molecules in UHV the bromine atom can be cleaved, and dehalogenation of the precursors occurs leading to gears structures **1** and **2**. As a result, the radical state of the de-halogenated molecules leads to a new metal-organic bond with the Au(111) substrate (Figure S6) that can serve as an center of rotation. To gain further insight in such molecule-substrate interactions, DFT calculations were performed. From Figure 3e, the DFT simulated STM image of gear **2** has a good agreement with the experimental image (Figure 3a), where it confirms the conformation of **2** and successful debromination on surface. Indeed, in the simulated STM image of precursor **4** (Figure 3b), the presence of the bromine atom pointing away from the surface (Figure 3d) is easily identified. Furthermore, DFT calculations (Figure 3f, g) reveal the adsorption geometry of gear **2** molecules on Au(111), with the central cyclopentadiene plane parallel to the surface. This highlights the likely contribution of the five carbon atoms of the ring to the bonding with the metal atoms underneath, as expected from the delocalized nature of the cyclopentadienyl radical. The adsorption energy is significantly lower for brominated precursor 4 (2.58 eV) than for the debrominated gear 2 (2.87 eV), pointing to the formation of a stronger bond for the later, in agreement with its observed anchoring.

The anchoring strategy was subsequently tested in lateral manipulation experiments to probe the possibility for gears **1** and **2** to undergo concentric motions. Surprisingly, with the same anchoring strategy, gear **1** fails to show concentric rotational motions (Figure 4) while most of

the gear **2** molecules reproducibly rotate (Figure 5). As discussed in the following, this observation further confirms that, more than a simple marker, such a *tert*-butyl group also plays an important role on facilitating the interaction with the tip during manipulation and stabilizing the molecule-gears on metal surfaces [29, 30], thus facilitating the rotation.

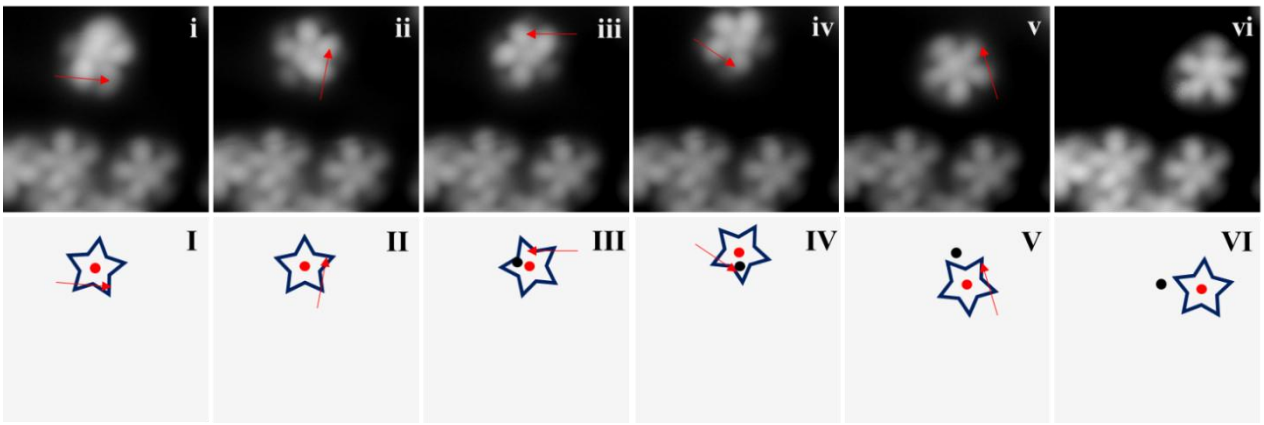

Figure 4. Non-concentric rotation of a single molecule-gear **1**. Red arrows indicate the trajectories of lateral manipulations (V = 10 mV, I = 8 pA; tunneling resistance = 1.25 GΩ) achieved by the STM tip. (i – ii) Only the first step of manipulation generated a concentric rotation. (iii – vi) The rest of manipulations induced both rotations and small lateral shifts. (I – VI) Corresponding schematic diagrams of the gear rotations (not in scale). Black and red dots indicate the lateral displacements before and after manipulations, respectively. All STM images (5 nm x 5 nm) were taken under the conditions of V = 500 mV and I = 7.2 pA.

Figure 4 shows a stepwise rotation sequence of gear **1** imaged by the STM. All lateral manipulations (red arrows) were applied in constant current mode. The STM captures images before and after each manipulation in all the following sequences. All the steps show successful movements induced by the STM tip, however, only step 1 (i – ii) shows a concentric rotation while the rest shows small lateral shifts with some degrees of rotations. During both imaging and

lateral manipulation, the molecules could be easily picked up by the STM tip at very low tunneling current (I = 8 - 10 pA). A total of five lateral manipulations were performed (see red arrows) where the tip apex travelled across one of the teeth towards the next tooth in constant current mode. Transmitting rotations between gear **1** molecules has been attempted, however, only movements like the ones reported in ref. [17] for a single HB-NBP molecule-gear have been observed, as shown in Figure S7.

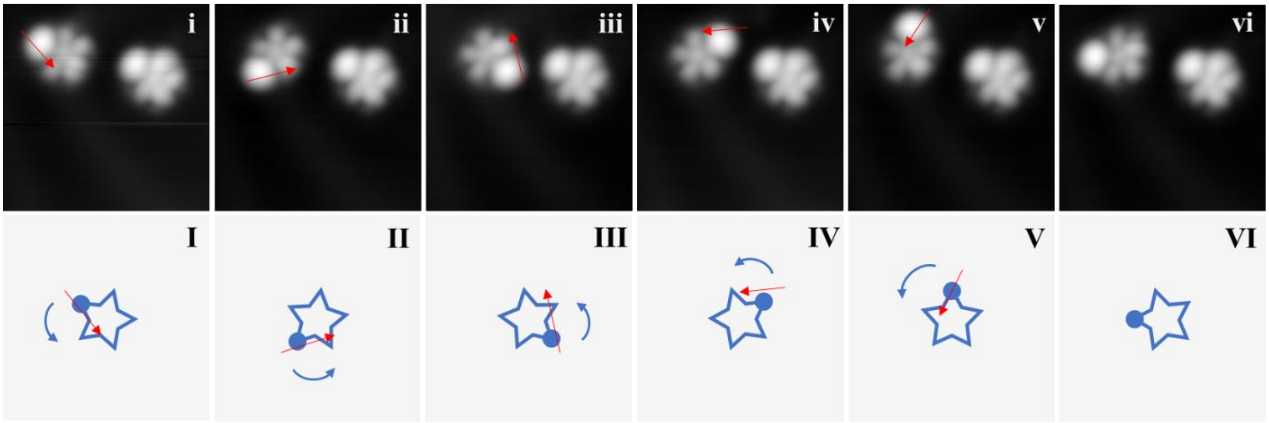

Figure 5. Rotation of a single molecule-gear **2**. Red arrows indicate the trajectories of lateral manipulations (V = 10 mV and I = 8 pA; tunneling resistance = 1.25 GΩ) achieved by the STM tip. (i - vi) Rotational sequence of a single molecule-gear **2**. The molecule on the right acts as a reference. (I – VI) Corresponding schematic diagrams of the gear rotations (not in scale). All STM images (6.5 nm x 6.5 nm) were taken under the conditions of V = 530 mV and I = 13 pA.

Figure 5 shows a step-by-step and complete rotation of a single molecule gear **2** in an anti-clockwise direction by five manipulations. All lateral manipulations (red arrows) were applied in constant-current mode. The rotational angles are in average 84° and we observed a maximum total rotation of 419°. Note that the rotations of the single gear are concentric, indicating that the

interaction between the cyclopentadienyl radical and the surface successfully and strongly anchors the gear at the pinning position determined by DFT calculations (See Figure 3).

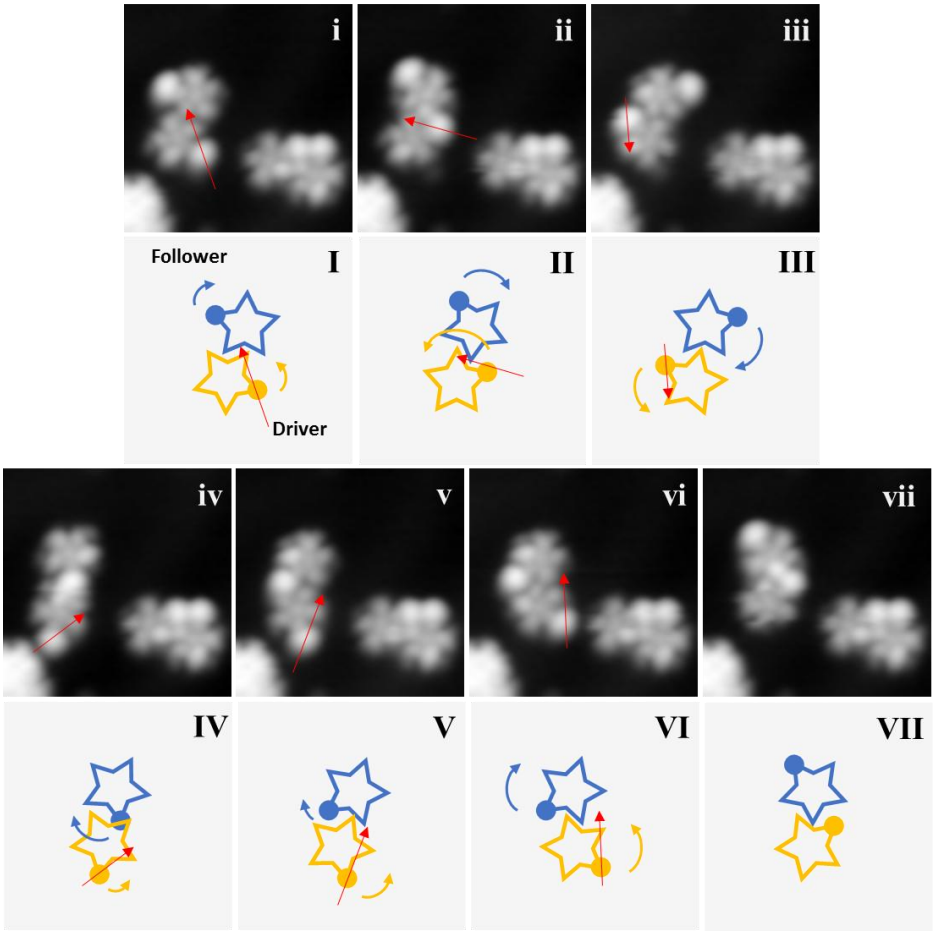

Figure 6. Stepwise collective rotational sequence between two single molecule-gears **2**. Red arrows indicate the trajectories of lateral manipulations (V = 10 mV and I = 14 pA; tunneling resistance = 0.71 GΩ) achieved by the STM tip. (i – vii) The rotations between two gear **2** molecules. The other two molecules on the right act as a reference and their motion sequence is shown in Figure S8. (I – VII) Corresponding schematic diagrams of the gear rotations (not in scale). All STM images (6.5 nm x 6.5 nm) were taken under the conditions of V = 530 mV and I = 13 pA.

Isolation of individual gear **2** molecules (Figures 5–7) was achieved by gently crashing the STM tip near a molecular island (Figure 2d). Smaller groups of 2–4 molecule trains formed after the tip crashing. Therefore, it was possible to obtain a sufficient amount of coupled gears. From Figure 6, a sequence of stepwise and complete rotations of two meshing molecule-gears is demonstrated. A sequence of six lateral manipulations are performed (See trajectories indicated by red arrows).

The average gear-to-gear distance in this case is 1.41 ± 0.05 nm, measured from center to center on the STM images. The minimum distance is about 1.30 nm (Figure 6ii) and the maximum distance is about 1.70 nm (Figure 6iv). Due to this method, we estimate an uncertainty of 0.05 nm in the distances and of 2° in the angles.

The STM tip drives the driver gear by interacting with the *tert*-butyl tooth in order to generate an anti-clockwise rotation. Simultaneously, such anti-clockwise rotation mechanically transmits to the follower gear. As a result, the follower gear rotates clockwise. From the whole sequence (Figure 6), each rotational angle is on average 83° for the driver and 68° for the follower; totally 499° for the driver and 410° for the follower (see Supplementary Information for further details). Interestingly, larger rotational angles between steps 2 – 3 (Figure 6ii – iii; angle: 122°) and 3 – 4 (Figure 6iii – iv; angle: 116°) are observed while the *tert*-butyl teeth of the gear directly interact with the phenyl rings of the other.

Such large gear-to-gear distance occurs when the tert-butyl group of the follower directly interacts with the other, possibly due to the larger molecular interactions and/or the larger size of the *tert-butyl* group.

Furthermore, a small lateral displacement (about 0.4 nm) of the driver gear is observed between steps 5 – 6 (Figure 6v – vi). Further information about the gear distance during the transmission of rotation is presented in the Supporting Information.

One additional step (Figure 6vi – vii) was needed to achieve a full rotation on the follower due to the insufficient motion between steps 5 – 6 (Figure 6v – vi; angle: 4°). It is worth to notice that as previous simulations [31-33] suggest, the follower can experience smaller rotational angles than the driver. Many degrees of freedom of the follower are activated while pushing on the driver as observed in ref. [17]. In other words, the collective rotational degrees of freedom of the follower, activated by the STM tip, are in competition with many other possible intramolecular mechanical modes.

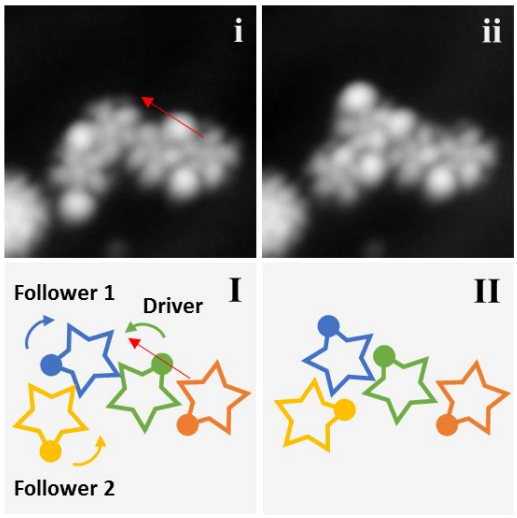

Figure 7. Stepwise collective rotational sequence between three single molecule-gears **2**. Red arrows indicate the trajectories of lateral manipulation (V = 10 mV and I = 14 pA; tunneling resistance = 0.71 GΩ) achieved by the STM tip. (i – ii) STM tip manipulation at the third gear as a driver induced a three-in-a-train collective rotation. The gear on the right side did not mesh with the driver, hence, no rotation was observed. (I – II) Corresponding schematic diagrams of

the gear rotations (not in scale). All STM images (6.5 nm x 6.5 nm) were taken under the conditions of V = 530 mV and I = 1.9 pA.

Transmitting a rotation along a train of gears is an essential prerequisite for the construction of molecular mechanical machines. To the best of our knowledge, there was no transmission of rotations realized between more than two molecule-gears [17]. Here, we present a collective transmission of rotation between three molecule-gears **2** (Figure 7). While manipulating (red arrow) the *tert*-butyl tooth of the third gear as a driver (Figure 7i) by the STM tip, we induced a step of transmission of rotation between three meshing gears. The scene is described as follows: an anticlockwise rotation from the driver (green) initiates a clockwise rotation for 75° at the follower 1 (blue), then simultaneously results to an anticlockwise rotation for 78° at the follower 2 for 104° (yellow) (Figure 7i – ii).. Before manipulation (Figure 7i), the gear-to-gear distance between driver and follower 1 is about 1.20 nm, and 1.26 nm between the two followers. After a step of rotation (Figure 7ii), we observe small lateral displacements happened for all the three gears that between driver and follower 1 is about 1.30 nm, and 1.38 nm between the two followers. Note that the gear on the right side (brown) did not mesh with the driver at a sufficient distance, hence, no rotation was observed. Nevertheless, no further rotation after this scenario was observed within the same train of molecules possibly due to the interlocking of *tert*-butyl groups between gears.

Comparison of the motions of the two proposed designs reveals that only gear **2** showed transmission of rotation up to three meshing gears. Given that the tunneling resistances are very similar (0.71 – 1.25 GΩ) during the manipulation of both gears in the constant-current mode, the driving potential energy increase are nearly the same in all rotations. In addition, assuming that the interactions between the bare phenyl rings from both gears **1** and **2** are the same, we suggest

that during STM manipulation, the presence of the *tert*-butyl group of gear **2** provides a more favorable tip-gear interaction than the planar phenyl ring of gear **1**.

In other words, the increase of potential energy induced by the tip manipulating the *tert*-butyl group of the driver allows the train of three gears to find a minimum energy path on the corresponding ground state potential energy surface (PES), and thus makes possible the transmission of rotation along the train. The end of the scenario indicates that after following this minimal energy path, a deep minimum energy well is existing on the PES of those three molecules interacting together which is stabilizing the final conformation imaged in Figure 7ii.

For assemblies of more than three molecule-gears in a train, we have not observed any successful transmission of rotation. A possible reason is that the tip-induced potential energy increase of the driver is not able in this case to excite the rotational degrees of freedom of the followers but is directed towards others degrees of freedom on the PES. Further optimization of the molecular design is therefore needed for building longer trains of gears working on a surface.

In conclusion, we have presented a sequence of rotation transmission along a train of gears up to three interlocked molecules. Our observations shed light on the challenges concerning the quality of the anchoring strategy, of the visualization by a chemical or a steric tag, and of tip-induced manipulation. These design rules are interdependent because a very specific energy path on the ground state potential energy surface of the train is needed to observe a transmission of rotation. For example, a steric *tert*-butyl tag can favor the tip-induced manipulation and stabilize the gear, but simultaneously hinder the further transmission of rotation. As a next challenge, the controllability of rotating a larger number of gears in a train is especially critical for the development of molecular mechanical machines, like mechanical calculators.

Methods

The brominated precursors of the PPCP-derived molecule-gears **1** and **2** were prepared in two steps from 2,3,4,5-tetraphenylcyclopentadienone by addition of the appropriate aryl lithium species followed by bromination of the intermediate alcohol (see Scheme 1). Precursor **3** incorporating a pyrimidinyl group ($C_{33}H_{23}BrN_2$) was obtained with a 53% overall yield as a mixture of three regioisomers, related to the location of the bromine atom on the different positions of the five-membered ring. According to the same synthetic sequence, precursor **4** displaying a 4-*tert*-butylphenyl moiety ($C_{39}H_{33}Br$) was prepared with a 63% yield, as a mixture of three regioisomers [34]. It is essential to note that, in each case, the three regioisomers of the precursor will give the same molecule as a unique isomer after debromination.

Both modified PPCP precursor **3** and **4** molecules were evaporated at 458 K and 441 K respectively for 30 s on a Au(111) surface kept at room temperature. Before evaporations, the samples were cleaned by subsequent cycles of Ar sputtering and annealing to 723 K. STM experiments were performed using a custom-built instrument operating at a low temperature of T = 5 K and ultrahigh vacuum ($p \approx 1 \times 10^{-10}$ mbar) conditions. All shown STM images were recorded in constant-current mode with the bias voltage applied to the sample.

All lateral manipulations were performed in constant current mode. Lateral manipulation procedure involves three steps: 1) vertically approaching the tip towards the molecules under a small bias and current to increase the tip-molecule interaction, 2) laterally driving the tip parallel to the surface in a precisely controlled trajectory, 3) retracting the tip to normal scanning position. Red arrows in all the manipulation sequences indicate trajectories of lateral manipulations, usually along one of the gear teeth (i.e. phenyl ring). The manipulation parameters are similar for different cases: V = 10 mV and I = 8 - 14 pA, tunneling resistance = 0.71 – 1.25 GΩ. The STM captures images before and after each manipulation in all the sequences.

DFT calculations have been performed using the VASP code [35]. Core electrons have been treated using the projector augmented-wave method [36, 37] and wave functions have been expanded using a plane-wave basis set with an energy cutoff of 400 eV. Exchange and correlation energies have been treated within the generalized gradient approximation in the PBE form [38]. Missing van der Waals interactions have been added using the Tkatchenko-Scheffler scheme [39]. The Au(111) surface has been modeled using a slab geometry with four layers in a 10x6√3 surface supercell and a vacuum region of ≈19 Å. Top two Au layers and the molecule have been relaxed until all the forces where smaller than 0.02 eV/Å.

STM topographic images have been simulated within the Tersoff-Hamann approximation [40, 41] using the method by Bocquet *et al* [42] as implemented in STMpw [43]. Adsorption energies have been calculated as

$$Ead = E(mol) + E(Au(111)) - E(mol@Au(111)),$$

where E(mol), E(Au(111)) and E(mol@Au(111)) are the energies of the gas-phase molecule, the gold surface, and the supported molecule, respectively.

ASSOCIATED CONTENT

Supporting Information.

The following file containing details on the chemical synthesis, additional experimental data, and additional theoretical results is available free of charge (PDF).

Author Contributions

All authors discussed the results and contributed to the manuscript. The manuscript was written through contributions of all authors. All authors have given approval to the final version of the manuscript.

ACKNOWLEDGMENT

This work was supported by the European Union Horizon 2020 FET open project "Mechanics with Molecules" (MEMO, Grant 766864), the University Paul Sabatier (Toulouse, France) and CNRS. This research was also partly supported by the JSPS KAKENHI grant in aid for Scientific Research on Innovative Areas "Molecular Engine (No.8006)" 18H05419. Y.G. thanks the MESR for a PhD Fellowship.

REFERENCES

1. Kassem, S.; van Leeuwen, T.; Lubbe, A. S.; Wilson, M. R.; Feringa, B. L.; Leigh, D. A., Artificial molecular motors. *Chemical Society Reviews* **2017,** *46* (9), 2592-2621.
2. Koumura, N.; Zijlstra, R. W. J.; van Delden, R. A.; Harada, N.; Feringa, B. L., Light-driven monodirectional molecular rotor. *Nature* **1999,** *401* (6749), 152-155.
3. Vale, R. D.; Milligan, R. A., The Way Things Move: Looking Under the Hood of Molecular Motor Proteins. *Science* **2000,** *288* (5463), 88.
4. Henningsen, N.; Franke, K. J.; Torrente, I. F.; Schulze, G.; Priewisch, B.; Rück-Braun, K.; Dokić, J.; Klamroth, T.; Saalfrank, P.; Pascual, J. I., Inducing the Rotation of a Single Phenyl Ring with Tunneling Electrons. *The Journal of Physical Chemistry C* **2007,** *111* (40), 14843-14848.
5. Manzano, C.; Soe, W. H.; Wong, H. S.; Ample, F.; Gourdon, A.; Chandrasekhar, N.; Joachim, C., Step-by-step rotation of a molecule-gear mounted on an atomic-scale axis. *Nature Materials* **2009,** *8* (7), 576-579.
6. Soe, W.-H.; Shirai, Y.; Durand, C.; Yonamine, Y.; Minami, K.; Bouju, X.; Kolmer, M.; Ariga, K.; Joachim, C.; Nakanishi, W., Conformation Manipulation and Motion of a Double Paddle Molecule on an Au(111) Surface. *ACS Nano* **2017,** *11* (10), 10357-10365.
7. Seldenthuis, J. S.; Prins, F.; Thijssen, J. M.; van der Zant, H. S. J., An All-Electric Single-Molecule Motor. *ACS Nano* **2010,** *4* (11), 6681-6686.
8. Moresco, F., Manipulation of large molecules by low-temperature STM: model systems for molecular electronics. *Physics Reports* **2004,** *399* (4), 175-225.
9. Kudernac, T.; Ruangsupapichat, N.; Parschau, M.; Maciá, B.; Katsonis, N.; Harutyunyan, S. R.; Ernst, K.-H.; Feringa, B. L., Electrically driven directional motion of a four-wheeled molecule on a metal surface. *Nature* **2011,** *479* (7372), 208-211.

10. Pawlak, R.; Meier, T.; Renaud, N.; Kisiel, M.; Hinaut, A.; Glatzel, T.; Sordes, D.; Durand, C.; Soe, W.-H.; Baratoff, A.; Joachim, C.; Housecroft, C.; Constable, E.; Meyer, E., Design and Characterization of an Electrically Powered Single Molecule on Gold. *ACS Nano* **2017,** *11*.
11. Liljeroth, P.; Repp, J.; Meyer, G., Current-Induced Hydrogen Tautomerization and Conductance Switching of Naphthalocyanine Molecules. *Science* **2007,** *317* (5842), 1203.
12. Auwärter, W.; Seufert, K.; Bischoff, F.; Ecija, D.; Vijayaraghavan, S.; Joshi, S.; Klappenberger, F.; Samudrala, N.; Barth, J. V., A surface-anchored molecular four-level conductance switch based on single proton transfer. *Nature Nanotechnology* **2012,** *7* (1), 41-46.
13. Zhao, A.; Li, Q.; Chen, L.; Xiang, H.; Wang, W.; Pan, S.; Wang, B.; Xiao, X.; Yang, J.; Hou, J. G.; Zhu, Q., Controlling the Kondo Effect of an Adsorbed Magnetic Ion Through Its Chemical Bonding. *Science* **2005,** *309* (5740), 1542.
14. Lauhon, L. J.; Ho, W., Single-Molecule Chemistry and Vibrational Spectroscopy: Pyridine and Benzene on Cu(001). *The Journal of Physical Chemistry A* **2000,** *104* (11), 2463-2467.
15. Gimzewski, J.; Joachim, C.; Schlittler, R. R.; Langlais, V.; Tang, H.; Johannsen, I., Rotation of a Single Molecule Within a Supramolecular Bearing. *Science* **1998,** *281*, 531-3.
16. Chiaravalloti, F.; Gross, L.; Rieder, K.-H.; Stojkovic, S. M.; Gourdon, A.; Joachim, C.; Moresco, F., A rack-and-pinion device at the molecular scale. *Nature Materials* **2007,** *6* (1), 30-33.
17. Soe, W.-H.; Srivastava, S.; Joachim, C., Train of Single Molecule-Gears. *The Journal of Physical Chemistry Letters* **2019,** *10* (21), 6462-6467.
18. Simpson, G. J.; García-López, V.; Daniel Boese, A.; Tour, J. M.; Grill, L., How to control single-molecule rotation. *Nature Communications* **2019,** *10* (1), 4631.
19. Schendel, V.; Borca, B.; Pentegov, I.; Michnowicz, T.; Kraft, U.; Klauk, H.; Wahl, P.; Schlickum, U.; Kern, K., Remotely Controlled Isomer Selective Molecular Switching. *Nano Letters* **2016,** *16* (1), 93-97.
20. Homberg, J.; Lindner, M.; Gerhard, L.; Edelmann, K.; Frauhammer, T.; Nahas, Y.; Valášek, M.; Mayor, M.; Wulfhekel, W., Six state molecular revolver mounted on a rigid platform. *Nanoscale* **2019,** *11* (18), 9015-9022.
21. Gao, L.; Liu, Q.; Zhang, Y. Y.; Jiang, N.; Zhang, H. G.; Cheng, Z. H.; Qiu, W. F.; Du, S. X.; Liu, Y. Q.; Hofer, W. A.; Gao, H. J., Constructing an Array of Anchored Single-Molecule Rotors on Gold Surfaces. *Physical Review Letters* **2008,** *101* (19), 197209.
22. Perera, U. G. E.; Ample, F.; Kersell, H.; Zhang, Y.; Vives, G.; Echeverria, J.; Grisolia, M.; Rapenne, G.; Joachim, C.; Hla, S. W., Controlled clockwise and anticlockwise rotational switching of a molecular motor. *Nature Nanotechnology* **2013,** *8* (1), 46-51.
23. Zhang, Y.; Kersell, H.; Stefak, R.; Echeverria, J.; Iancu, V.; Perera, U. G. E.; Li, Y.; Deshpande, A.; Braun, K. F.; Joachim, C.; Rapenne, G.; Hla, S. W., Simultaneous and coordinated rotational switching of all molecular rotors in a network. *Nature Nanotechnology* **2016,** *11* (8), 706-712.
24. Bartels, L.; Meyer, G.; Rieder, K. H., Basic Steps of Lateral Manipulation of Single Atoms and Diatomic Clusters with a Scanning Tunneling Microscope Tip. *Phys. Rev. Lett.* **1997,** *79* (4), 697-700.
25. Field, L. D.; Lindall, C. M.; Masters, A. F.; Clentsmith, G. K. B., Penta-arylcyclopentadienyl complexes. *Coordination Chemistry Reviews* **2011,** *255* (15), 1733-1790.

26. Kammerer, C.; Rapenne, G., Scorpionate Hydrotris(indazolyl)borate Ligands as Tripodal Platforms for Surface-Mounted Molecular Gears and Motors. *European Journal of Inorganic Chemistry* **2016,** *2016* (15-16), 2214-2226.
27. Erbland, G.; Abid, S.; Gisbert, Y.; Saffon-Merceron, N.; Hashimoto, Y.; Andreoni, L.; Guérin, T.; Kammerer, C.; Rapenne, G., Star-Shaped Ruthenium Complexes as Prototypes of Molecular Gears. *Chemistry – A European Journal* **2019,** *25* (71), 16328-16339.
28. Grill, L.; Dyer, M.; Lafferentz, L.; Persson, M.; Peters, M. V.; Hecht, S., Nano-architectures by covalent assembly of molecular building blocks. *Nature Nanotechnology* **2007,** *2* (11), 687-691.
29. Otero, R.; Hümmelink, F.; Sato, F.; Legoas, S. B.; Thostrup, P.; Lægsgaard, E.; Stensgaard, I.; Galvão, D. S.; Besenbacher, F., Lock-and-key effect in the surface diffusion of large organic molecules probed by STM. *Nature Materials* **2004,** *3* (11), 779-782.
30. Schunack, M.; Linderoth, T. R.; Rosei, F.; Lægsgaard, E.; Stensgaard, I.; Besenbacher, F., Long Jumps in the Surface Diffusion of Large Molecules. *Physical Review Letters* **2002,** *88* (15), 156102.
31. MacKinnon, A., Quantum gears: a simple mechanical system in the quantum regime. *Nanotechnology* **2002,** *13* (5), 678-681.
32. Zhao, R.; Qi, F.; Zhao, Y.-L.; Hermann, K. E.; Zhang, R.-Q.; Van Hove, M. A., Interlocking Molecular Gear Chains Built on Surfaces. *The Journal of Physical Chemistry Letters* **2018,** *9* (10), 2611-2619.
33. Lin, H. H.; Croy, A.; Gutierrez, R.; Joachim, C.; Cuniberti, G., Mechanical Transmission of Rotational Motion between Molecular-Scale Gears. *Physical Review Applied* **2020,** *13* (3), 034024.
34. Vives, G.; Rapenne, G., Directed synthesis of symmetric and dissymmetric molecular motors built around a ruthenium cyclopentadienyl tris(indazolyl)borate complex. *Tetrahedron* **2008,** *64* (50), 11462-11468.
35. Kresse, G.; Furthmüller, J., Efficiency of ab-initio total energy calculations for metals and semiconductors using a plane-wave basis set. *Computational Materials Science* **1996,** *6* (1), 15-50.
36. Blöchl, P. E., Projector augmented-wave method. *Physical Review B* **1994,** *50* (24), 17953-17979.
37. Kresse, G.; Joubert, D., From ultrasoft pseudopotentials to the projector augmented-wave method. *Physical Review B* **1999,** *59* (3), 1758-1775.
38. Perdew, J. P.; Burke, K.; Ernzerhof, M., Generalized Gradient Approximation Made Simple. *Physical Review Letters* **1996,** *77* (18), 3865-3868.
39. Tkatchenko, A.; Scheffler, M., Accurate Molecular Van Der Waals Interactions from Ground-State Electron Density and Free-Atom Reference Data. *Physical Review Letters* **2009,** *102* (7), 073005.
40. Tersoff, J.; Hamann, D. R., Theory and Application for the Scanning Tunneling Microscope. *Physical Review Letters* **1983,** *50* (25), 1998-2001.
41. Tersoff, J.; Hamann, D. R., Theory of the scanning tunneling microscope. *Physical Review B* **1985,** *31* (2), 805-813.
42. Bocquet, M.-L.; Lesnard, H.; Monturet, S.; Lorente, N., Theory of Elastic and Inelastic Electron Tunneling. In *Computational Methods in Catalysis and Materials Science*, 2009; pp 199-219.
43. Lorente, N.; Robles, R. *STMpw*, v1.0b2; Zenodo: 2019.